

Spatial Cascaded Clustering and Weighted Memory for Unsupervised Person Re-identification

Jiahao Hong Jialong Zuo Chuchu Han Ruochen Zheng Ming Tain
Changxin Gao Nong Sang
{hongjiahao, jlongzuo, cch, cgao, zhengruochen, tainming, nsang}@hust.edu.cn

Abstract

Recent unsupervised person re-identification (re-ID) methods achieve high performance by leveraging fine-grained local context. These methods are referred to as part-based methods. However, most part-based methods obtain local contexts through horizontal division, which suffer from misalignment due to various human poses. Additionally, the misalignment of semantic information in part features restricts the use of metric learning, thus affecting the effectiveness of part-based methods. The two issues mentioned above result in the under-utilization of part features in part-based methods. We introduce the Spatial Cascaded Clustering and Weighted Memory (SCWM) method to address these challenges. SCWM aims to parse and align more accurate local contexts for different human body parts while allowing the memory module to balance hard example mining and noise suppression. Specifically, we first analyze the foreground omissions and spatial confusions issues in the previous method. Then, we propose foreground and space corrections to enhance the completeness and reasonableness of the human parsing results. Next, we introduce a weighted memory and utilize two weighting strategies. These strategies address hard sample mining for global features and enhance noise resistance for part features, which enables better utilization of both global and part features. Extensive experiments on Market-1501 and MSMT17 validate the proposed method’s effectiveness over many state-of-the-art methods.

1. Introduction

Most recent unsupervised person re-identification methods [3, 8, 11, 20, 34, 39, 44, 45] have adopted an alternating two-stage training framework: 1) clustering samples in feature space to provide pseudo labels for training. 2) training the network under the supervision of pseudo labels generated by clustering. However, these methods are still susceptible to the limitations of clustering algorithms, as imperfect

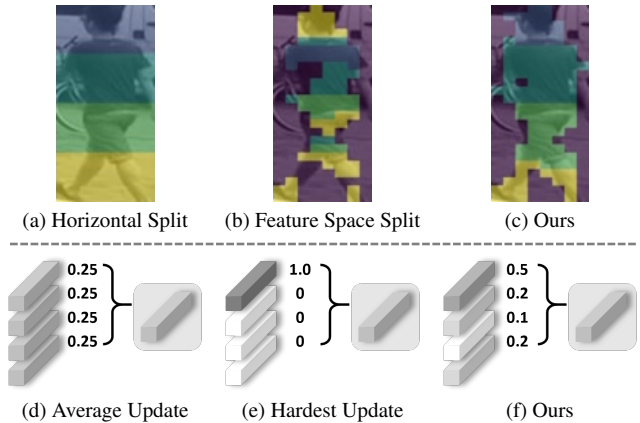


Figure 1. Method differences illustration. The first row shows the difference in fine-grained split between existing methods and ours. Our method incorporates spatial information to correct the feature space, making the clustering results more coherent. The second row shows the difference in memory update strategy. Our method balances hard sample mining and noise resistance in the memory module through weighting.

clustering methods may introduce noise.

The approach to addressing this issue categorizes existing methods into two types: one that utilizes only global information [12, 13, 32, 44, 45, 49] and the other that simultaneously uses global and local information [8]. These two types of methods enhance the reliability and stability of clustering by leveraging different sources of information. The singularity of global features limits the first type of method, so we focus on the second type of method, which can leverage more information, namely part-based methods. Although part-based methods have achieved good results thanks to rich fine-grained information, their local partitioning methods are still too coarse [8]. Furthermore, due to the differences in network structures and task settings, the direct application of previous human parsing methods may be limited [50], necessitating further corrections and improvements.

Additionally, due to the absence of semantic alignment

in local partitioning in previous methods, metric learning cannot be effectively applied to fine-grained local features [8, 18], leading to limited network performance. Furthermore, previous research on metric learning has primarily focused on global features and has not considered the subtle differences between part and global features. Therefore, directly applying the previous memory module to local features has limited effectiveness.

In response to the problems above, we propose the Spatial Cascaded Clustering and Weighted Memory (SCWM) method. SCWM can automatically parse and align human body parts, and enable a more comprehensive utilization of global and local information. Building upon the existing part-based approach, our SCWM consists of a spatial cascaded clustering (SCC) and a weighted memory (WM).

Specifically, building upon previous work [7, 36, 50], we utilize cascaded clustering as the pseudo parsing mask generator but enhance it through foreground and space corrections. In the first step, previous methods distinguish foreground and background by the strength of the feature map response. Still, they have ignored the neural network’s tendency to prioritize the most salient regions, which can lead to regular foreground being mistaken for background. To address this issue, we cluster the parts with significantly high responses in the foreground separately. This helps avoid excessively high responses raising the average response of the foreground cluster, which might result in foreground with smaller responses being mistaken as background. In the second step, previous methods only cluster feature vectors in feature space, disregarding their positional relationships in spatial space. As a result, previous methods may incorrectly cluster similar features from different parts. Therefore, we opt for Agglomerative Clustering and utilize a precomputed distance matrix to incorporate spatial information. Given that a person’s features in space are often not significantly distant, we assign an infinite distance between vectors if their spatial distance exceeds the threshold after calculating the distances between vectors in feature space. This spatial constraint significantly enhances the reliability of our clustering.

After aligning part features, we can employ metric learning to part features. However, initially designed for global features, the previous memory module [9, 13] shows limited performance when directly applied to part features. Therefore, we propose a weighted memory that simultaneously adapts to global and part features. Its flexible weighted update allows it to balance noise suppression and hard example mining. Given the differences between global and local features, we proposed two weighting strategies. For part features, due to the need for noise suppression, harder samples are considered to contain more noise. Therefore, the weights for hard samples should be smaller than simple samples. Conversely, for global features, the weighting for

harder samples should be higher to construct samples that are more conducive to network learning. Additionally, previous methods only considered individual part spaces separately, neglecting the relationships between different part spaces. To address this limitation, we introduced a part separation loss, which aims to encourage part features to emphasize their unique information and enhance the overall diversity of part features.

Our contributions can be summarized as follows:

- We improve the existing cascaded clustering by foreground correction and space correction.
- We introduce a weighted memory and propose two weighting strategies to balance learning hard samples and reducing noise.
- Extensive experimental results with superior performance against the state-of-the-art methods demonstrate the effectiveness of the proposed method.

2. Related Work

Part-based person re-ID. Part-based approaches for person re-ID leverage fine-grained information on human body parts, such as features from rigid stripe [29, 46], auto-localization [18, 41], attention [2, 19, 27, 40], and extra semantics [14, 21, 22, 24, 26, 28, 48]. While part-based methods have demonstrated significant performance, the coarse part segmentation methods have limited these attempts to utilize part features. In visible-infrared re-ID, MPANet [36] proposed using lightweight convolutional layers to divide the feature map into different parts. However, the division results were not ideal due to the lack of clear semantic guidance. ISP [50] introduced a self-learning human parsing method for the first time in supervised re-ID, which is used for pixel-level semantic part feature extraction. Recent work has also continued this line of thinking. SOLIDER [7] employs semantic segmentation-generated masks of human body parts for self-supervised re-ID to perform image masking operations. What mainly sets our method apart from these is that when parsing human body parts, we consider the similarity between pixels in the feature space and the inherent continuity and separability of a person’s body parts in spatial space.

Memory module. By establishing a memory module [1, 6, 17, 25, 30, 38, 42], contrastive learning [15] provides an efficient metric learning strategy in which the stored features can significantly reduce the difficulty of obtaining positive and negative sample pairs. Moco [17] has established a memory module for online updates of all sample features, significantly expanding the search scope for negative samples and overcoming the previous limitation of finding negative samples within a single batch. SpCL [13] builds a memory module for both clustered samples and unclustered outliers. MCRN [37] proposes a memory module that can

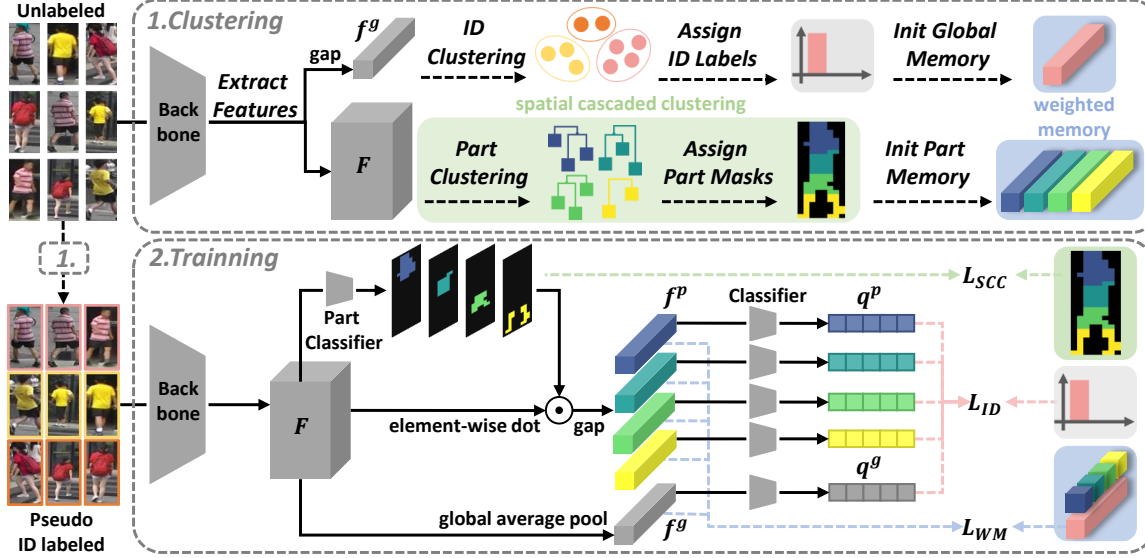


Figure 2. Framework of the proposed Spatial Cascaded Clustering and Weighted Memory (SCWM) method. The areas and lines annotated in light green represent the spatial cascaded clustering, while the areas and lines annotated in light blue represent the weighted memory.

store multiple centers for a cluster, modeling the overall features of a cluster by considering information from multiple centers. CCL [9] proposed a hardest sample updating strategy for the memory module. However, the method described above only considered global features, and the update strategy of the memory module was relatively simplistic, lacking the ability to adapt to current local features. Therefore, we proposed a weighted memory that can balance hard example mining and noise suppression through flexible weighted updates.

3. Method

In this section, we begin with introducing our overall framework in Sec. 3.1. Then, we discuss the spatial cascaded clustering in detail in Sec. 3.2. Next, we introduce the weighted memory and the two weighting strategies in Sec. 3.3. Finally, we provide a brief overview of the adopted classification constraints and the overall object function of the model in Sec. 3.4.

3.1. Overall Framework

We build our framework based on the current mainstream clustering-based method. All the following discussions will revolve around the two steps of the clustering-based method. The overall illustration is shown in Fig. 2.

Clustering stage. Firstly, we have an unlabeled dataset $\{x_i\}_{i=1}^N$ and need to extract their features. Here we freeze the parameter of the backbone network f_θ and use it to extract each sample’s feature map F , global feature f^g , and part features $\{f^{p_k}\}_{k=1}^l$. F is the output result of the last layer of the backbone. f^g is the global average pooling re-

sult of F . For part features f^{p_k} , we first use the backbone’s part classifier $G(\cdot)$ to predict every part of the feature map. Then, we multiply these predicted part masks with the feature map and perform global average pooling to obtain part features of each part. The formulas are shown below:

$$\begin{aligned} F &= f_\theta(x), \\ f^g &= GAP(F), \\ f^{p_k} &= GAP(G(F)_k \cdot F), k = 1, 2, \dots, l, \end{aligned} \quad (1)$$

where l is the number of parts in which the background is considered as one part, and $G(\cdot)$ consists of a 3×3 conv layer followed by a softmax function. Secondly, we generate the required pseudo ID labels and pseudo parsing masks. We use DBSCAN [10] clustering for all samples to assign a pseudo ID label to each cluster, denoted as $\{y_i\}_{i=1}^N$. For each sample, we apply cascaded clustering with foreground and space corrections to each feature map to obtain pseudo parsing masks, denoted as $M = [M_1, M_2, \dots, M_l]$. Finally, according to the pseudo ID labels, we individually initialize global and part memories with average cluster centroid.

Training stage. We use the pseudo labels provided by the clustering stage to train the network during the training stage. Firstly, we extract the features for each sample following the same steps as in the clustering stage. Among them, we denote the predicted part masks generated by the part classifier as $P = [P_1, P_2, \dots, P_l]$. Secondly, for the global feature and each part feature, we use separate classifiers to predict their categories vectors q^g and $\{q^{p_k}\}_{k=1}^l$. Finally, we conduct parsing loss L_{SCC} , metric learning loss L_{WM} , and classification loss L_{ID} on network f_θ .

3.2. Spatial Cascaded Clustering

Current unsupervised part-based person re-ID methods are constrained by misaligned part partitioning [8]. Therefore, we introduce self-learning human parsing with spatial cascaded clustering to enhance the accuracy of part features. The difference is that, as previous methods applied directly to unsupervised tasks resulted in foreground omissions and spatial confusions, we specifically proposed foreground and space correction to address these two issues.

In the first step of cascaded clustering, upon observation, the feature map F responses are consistently more significant for the foreground than the background [23, 50]. More importantly, some regions often have more salient responses within the foreground. However, due to the enormous responses of these salient regions, there is a risk of misclassifying foreground regions with smaller responses as background. Therefore, to mitigate the impact of salient regions on foreground judgment, we treat these regions as a distinct class during clustering. Hence, we adopt a three-class K-Means to divide the feature map F into three parts: salient foreground $\{F_{sf}\}$, regular foreground $\{F_{rf}\}$, and background $\{F_b\}$, based on the magnitude of the feature vectors.

In the second step of cascaded clustering, we employ Agglomerative Clustering with a precomputed distance matrix adjusted by spatial information. This approach addresses the limitations of existing methods that do not utilize spatial information. To explore the distance relationships between the vectors at each position in the feature map and all other vectors, we denote the c -dimension vector at each position in the feature map as v . First, for all vectors in foreground $\{F_{sf}\} \cup \{F_{rf}\}$, we compute their distance matrix in spatial space and feature space, denoted as D_s and D_f . Then, we set the distance in the feature space to infinity for vector pairs that are too far apart in spatial space, preventing confusion about a person’s semantic features. Finally, we cluster $\{v|v \in \{F_{sf}\} \cup \{F_{rf}\}\}$ into $l - 1$ parts $[M_1, M_2, \dots, M_{l-1}]$ based on the corrected distance matrix D :

$$D = \begin{cases} D_f(v_A, v_B), & \text{if } D_s(v_A, v_B) < \eta, \\ \infty, & \text{if } D_s(v_A, v_B) \geq \eta, \end{cases} \quad (2)$$

where v_A and v_B represent two vectors in $\{F_{sf}\} \cup \{F_{rf}\}$, η is the threshold that determines distances that are considered too far apart in spatial space, l is the total number of parts. The indices of the part clusters are arranged in descending order of the heights of the cluster centers. The background part M_l is $\{F_b\}$. To prevent abrupt changes in pseudo labels caused by variations in clustering between epochs, we employ the idea of momentum updating to smooth the pseudo parsing masks:

$$\widetilde{M} \leftarrow \gamma \widetilde{M} + (1 - \gamma)M, \quad (3)$$

where γ is the momentum factor, \widetilde{M} is the smoothed pseudo parsing masks.

Next, in the training stage, we consider the pseudo parsing masks as supervision to guide the learning of the part prediction:

$$L_{parsing} = -\widetilde{M} \log(P). \quad (4)$$

Furthermore, to ensure that different part masks can focus on distinct information, we use diversity loss to prevent the degradation of part masks:

$$L_{diversity} = \frac{2}{l(l-1)} \sum_{i=1}^{l-1} \sum_{j=i+1}^l \sum_{(x,y)} (P_i \cdot P_j), \quad (5)$$

where P_i and P_j mean the i -th and j -th predicted part mask, (x, y) means the point in mask, \cdot is element-wise multiplication. Then, the loss of spatial cascaded clustering is given by:

$$L_{SCC} = L_{parsing} + L_{diversity}. \quad (6)$$

3.3. Weighted Memory

Previous part-based methods do not apply metric learning to part features because the part features are not aligned [29]. Now, after self-learning human parsing, the body parts of different individuals are semantically aligned, and we can employ metric learning for part features. Recent metric learning approaches [9, 13, 45] often employ a memory module to expand the search range for positive and negative samples in contrastive loss. However, these methods do not utilize part features, and their memory modules designed for global features have limited effectiveness when directly applied to part features. Therefore, we propose the weighted memory and two weighting strategies after exploring the differences between global and part features.

Specifically, in the clustering stage, we utilize K-nearest neighbors (kNN) similarity to measure the difficulty level of a specific feature within a sample. For the part feature of a sample, its difficulty level is determined by the Intersection over Union (IoU) between its K-nearest neighbors and the K-nearest neighbors of the sample’s global features. As for global feature, its difficulty level is the average of all the difficulty levels of its sample’s part features. We denote α as the difficulty level:

$$\alpha^{p_k} = \frac{kNN(f^g) \cap kNN(f^{p_k})}{kNN(f^g) \cup kNN(f^{p_k})}, \quad (7)$$

$$\alpha^g = \frac{1}{l} \sum_{k=1}^l \alpha^{p_k}.$$

Intuitively, a large α^{p_k} implies that the part feature is similar to the global feature, indicating that the information contained in the part feature is reliable and its difficulty level should be low. For a small α^g , it indicates that the

global feature does not fit well with the surrounding samples, suggesting that it contains feature information not yet accounted for in the current cluster. Therefore, its difficulty level should be high. In summary, the difficulty coefficient of global features should have an opposite trend to the α^g , while the difficulty coefficient of part features should have the same trend as the α^{pk} . So when updating memory, we assign $1 - \alpha^g$ for each global feature. In contrast, we assign α^{pk} for each part feature. We use $l1$ -normalization in a batch to obtain the final sample weights, ensuring the stable update of class centroids:

$$\omega^g = \frac{1 - \alpha^g}{\sum 1 - \alpha_i^g}, \quad \omega^{pk} = \frac{\alpha^{pk}}{\sum \alpha_i^{pk}}, \quad (8)$$

where α represents an individual sample's difficult level, while $\sum \alpha_i$ is the sum within a batch. Then, the momentum update formula for the weighted memory can be summarized in the following form:

$$\begin{aligned} \forall f^g \in C_j^g, c_j^g &\leftarrow mc_j^g + (1 - m)\omega^g f^g, \\ \forall f^{pk} \in C_j^{pk}, c_j^{pk} &\leftarrow mc_j^{pk} + (1 - m)\omega^{pk} f^{pk}, \end{aligned} \quad (9)$$

where C_j^g and C_j^{pk} respectively stand for the set of global and k -th part features extracted from images of j -th cluster, c_j^g and c_j^{pk} are the cluster centroids of global and k -th part features from j -th cluster, m is the momentum factor.

Next, in the training stage, we modified the ClusterNCE loss [9] into a weighted form:

$$\begin{aligned} L_{wNCE} = &-\log \frac{\omega^g \cdot \exp(f^g \cdot c_+^g / \tau)}{\sum_{j=1}^{N_C} \exp(f^g \cdot c_j^g / \tau)} \\ &+ \frac{1}{l} \sum_{k=1}^l -\log \frac{\omega^{pk} \cdot \exp(f^{pk} \cdot c_+^{pk} / \tau)}{\sum_{j=1}^{N_C} \exp(f^{pk} \cdot c_j^{pk} / \tau)}, \end{aligned} \quad (10)$$

where τ is temperature factor, N_C is the number of clusters, c_+ is the centroid of the cluster to which f belongs and c_j is centroid of other cluster.

Moreover, given that different part features of the same individual should not overlap, we design a part separation loss in feature space:

$$L_{sep} = -\frac{1}{l} \sum_{k=1}^l \log \frac{\exp(f^{pk} \cdot c_+^{pk} / \tau)}{\sum_{j=1}^l \exp(f^{pk} \cdot c_j^{pk} / \tau)}, \quad (11)$$

where c_+^{pk} represents the cluster centroid of the j -th part feature of the samples in the cluster to which f belongs.

Then, the loss of the weighted memory is given by:

$$L_{WMM} = L_{wNCE} + L_{sep}. \quad (12)$$

3.4. Part-based Classification

Part-based classification methods have undergone significant development [8, 29, 33]. We follow the recent PPLR

[8] methods to design the classification constraints but explain them from a new perspective.

For a part feature, the lower its kNN similarity with the global feature, the more likely the part feature is noise. Therefore, its classification should not belong to any existing class. In formulaic terms, this can be seen as a form of weighted label smoothing, with the weighting factor being the sample difficulty coefficient:

$$y_i^{pk} = \alpha^{pk} y_i + (1 - \alpha^{pk}) uni, \quad (13)$$

where uni is a uniform vector representing a class label indicating that the feature does not belong to any class.

A form of knowledge distillation is needed for a global feature to incorporate the information from part features. This is reflected in the class labels by proportionally weighting the outputs of the part feature classifier to the global feature label:

$$y_i^g = \beta y_i + (1 - \beta) \tilde{\omega}_i^{pk} q_i^{pk}, \quad (14)$$

where β is a hyper-parameter that controls the degree of knowledge distillation, $\tilde{\omega}^{pk} = \frac{\exp(\alpha^{pk})}{\sum_k \exp(\alpha^{pk})}$ is the weight that determines the proportion of each part.

Then, the classification loss can be summarized as follows:

$$L_{ID} = -y_i^g \log(q_i^g) + \frac{1}{l} \sum_{k=1}^l -y_i^{pk} \log(q_i^{pk}). \quad (15)$$

Overall object function. The overall loss function of our methods is then:

$$L = L_{SCC} + L_{WMM} + L_{ID}. \quad (16)$$

4. Experiment

4.1. Datasets and Evaluation Protocols

We evaluate our proposed method on Market-1501 [47] and MSMT17 [35]. Market-1501 includes 32,668 images of 1,501 identities with 6 camera views, 12,936 images of 751 identities for training, and 19,732 images of 750 identities for testing. MSMT17 is a more challenging dataset comprising 126,441 images of 4,101 person identities captured from 15 cameras. The training set has 32,621 images of 1,041 identities, and the test set has 93,820 images of 3,060 identities. We use mean average precision (mAP) and cumulative matching characteristic (CMC) Rank-1, Rank-5, Rank-10 accuracies as the evaluation metrics. There are no postprocessing operations in testing, such as reranking.

4.2. Implementation Details

All our experiments were conducted on four 2080Ti. The backbone of our Re-ID model is ResNet-50 [16] pretrained

Methods	Market-1501		MSMT17	
	mAP	R1	mAP	R1
baseline	86.6	94.5	46.1	73.4
+ L_{wNCE}	87.2	94.4	47.2	74.6
+ L_{WM}	87.4	94.8	47.9	76.1
+ $L_{WM} + L_{parsing}$	84.4	93.5	41.4	70.0
+ $L_{WM} + L_{SCC}$	87.5	94.9	49.1	76.5

Table 1. Ablation study of each component in our proposed spatial cascaded clustering and weighted memory method.

on SYNTH-PEDES [51]. We remove all the layers after the fourth bottleneck of the backbone network and set the stride of the first convolution layer of the fourth bottleneck to 1. We append a global average pooling layer and a 3×3 convolution layer as the part classifier after the backbone. We add a batch normalization layer and l_2 -normalization layer to obtain 2048-dimension features. The person images are resized to 384×128 . Adam with weight decay of $5e-4$ is adopted for training. The initial learning rate is set to $3.5e-4$ and decreased by 10 after every 20 epochs. We train for a total 60 epochs and 400 iterations for each epoch. Following previous work [8, 13, 37, 45], we employ DBSCAN based on Jaccard distance with k-reciprocal encoding for clustering. The search radius in DBSCAN is set to 0.5 in Market-1501 and 0.7 in MSMT17. The number of parts is set to 4 in Market-1501 and 7 in MSMT17. The semantic parsing label update factor γ is set to 0.2 and decreases to 0 after 20 epochs. The memory update factor m is set to 0.2. The temperature τ is set to its default value of 0.05. The part distillation parameter β is set to 0.35.

4.3. Ablation Study

To validate the effectiveness of our method, we conduct detailed comparative experiments on Market-1501 and MSMT17. We adopt Part-based Pseudo Label Refinement [8] with backbone changed to SYNTH-PEDES pretrained ResNet-50 as the baseline for our experiment. We verify the effectiveness of the proposed methods: spatial cascaded clustering (SCC) and weighted memory (WM). In conclusion, our method improves mAP of the baseline by 0.9% and 3.0% on Market-1501 and MSMT17, respectively.

Effectiveness of spatial cascaded clustering. By comparing the results of Tab. 1 and Tab. 2, we can observe the effectiveness of SCC. Thanks to our proposed foreground and space corrections, SCC can better extract part features of the person based on the similarity of feature vectors in feature space and spatial space. It improves the situation of semantic misalignment at the feature level. To demonstrate the effectiveness of our proposed improved cascade clustering, we visualize the parsing results given by the original, the foreground-corrected, the space-corrected, and the foreground and space-corrected cascade clustering methods, re-

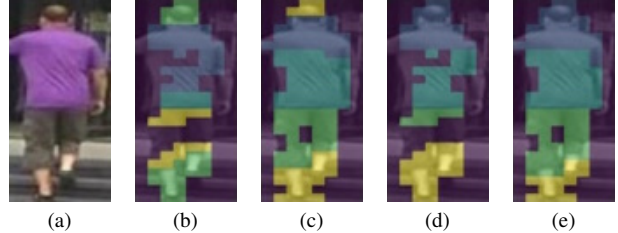


Figure 3. Visualization of pseudo parsing masks: (a) Input image; (b) origin cascaded clustering; (c) origin with foreground correction; (d) origin with space correction; (e) our foreground and space corrected clustering.

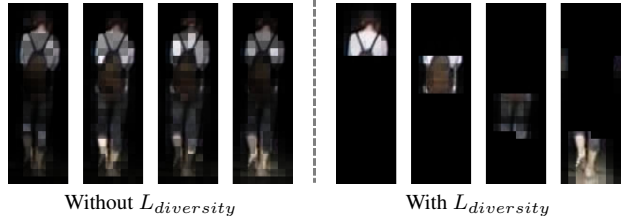


Figure 4. Visualization of predicted parsing masks. Without $L_{diversity}$, the predicted parsing masks the part classifier generates may degrade.

spectively. As shown in Fig. 3, our two improvements allow cascade clustering to obtain more complete foreground information and parsing more consistent with spatial relationships. The origin parsing results often exhibit partial omissions and confusion between semantic parts. The possible reason is that the original cascaded clustering is applied to feature maps extracted by HRNet [50]. Compared to the highly abstract feature maps of ResNet50, HRNet low-dimensional features are better suited for parsing tasks. So, when applied to ResNet50 feature maps, the original cascade clustering performs poorly. Another critical element in SCC is the $L_{diversity}$ loss. We also visualize the person parsing masks generated by the part classifier before and after using $L_{diversity}$ in Fig. 4. As can be seen from the figure, without $L_{diversity}$, the parsing masks generated by the part classifier tend to be the same for each part, which significantly damages the diversity of part features.

Effectiveness of weighted memory. By comparing the results of Tab. 1 and Tab. 3, we can observe the effectiveness of WM. The comparative experiment Tab. 3 is conducted under completely identical and comprehensive conditions, with the only change being replacing the memory module update strategy with average and hardest [9] updates. From Tab. 3, it can be seen that both the average update strategy and the hardest update strategy perform worse than our weighted update strategy. The average update strategy may be effective in most cases, but its effectiveness is limited due to its lack of focus on challenging sample exploration and noise suppression. The hardest update strategy provides an approach that focuses on exploring hard samples. However,

Methods	Market-1501		MSMT17	
	mAP	R1	mAP	R1
cascaded clustering	86.2	94.4	48.8	75.9
foreground correction	86.9	95.1	48.7	76.0
space correction	86.5	94.4	49.3	77.0
both correction	87.5	94.9	49.1	76.5

Table 2. Comparison of different parsing methods for part feature extraction.

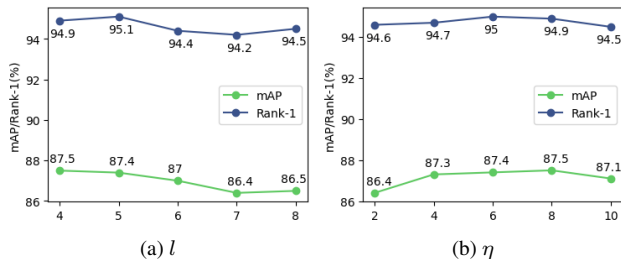


Figure 5. Parameter analysis of η and l on Market-1501.

the most hard samples will likely become the noise that pollutes the cluster centroid in the case of more noise samples. Our weighted update strategy lies between average updates and hardest updates. It neither treats all samples equally nor favors any one sample. Therefore, it can balance noise suppression and hard sample mining.

Parameter Analyse. We analyze two parameters in our method: the distance threshold η and the part numbers l in spatial cascaded clustering. We keep one parameter constant and adjust the other parameter for experimentation, and the results are in Fig. 5. A smaller η value will make the clustering conditions more stringent. When η is too small, clustering may absorb some vectors with a large spatial distance, causing the spatial constraints to become ineffective. Similarly, when η is too large, it is equivalent to having no spatial constraints. As shown in Fig. 5, it can be observed that when η is relatively large or small, there is a slight decrease in the mAP metric. Another critical parameter is part number l . On Market-1501, the best performance is achieved when $l = 4$. That is, the foreground is divided into three parts. This result is similar to previous work [50]. The probable reason is that in the Market-1501 dataset, people’s clothing is relatively unified, mainly divided into tops, bottoms, and shoes, and the clothing colors are vibrant. Therefore, additional personal items such as backpacks, handbags, bicycles, etc., may not significantly influence the classification. However, on MSMT17, the best performance is achieved when $l = 7$. This may be due to the prevalence of occlusions and incomplete cropping in person images within this dataset.

Clustering Quality. We visualize the baseline’s and our clustering results in Fig. 6. Due to the different poses of the person, the top horizontal partitioning used by the

Methods	Market-1501		MSMT17	
	mAP	R1	mAP	R1
average update	87.2	94.7	48.7	76.0
hardest update	87.4	95.1	48.3	75.6
weighted update	87.5	94.9	49.1	76.5

Table 3. Comparison of different update strategies for memory module.

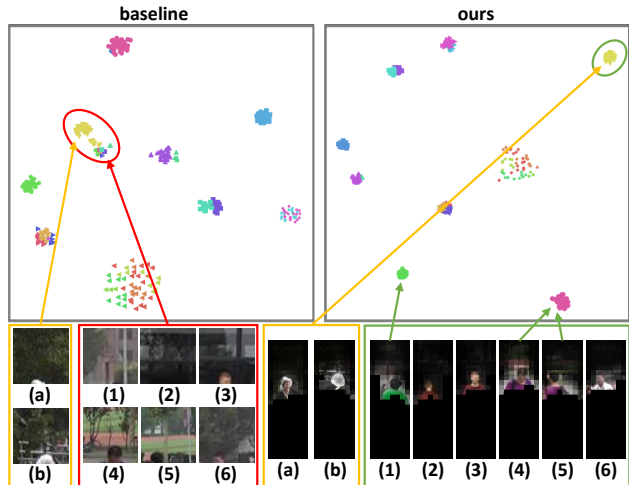


Figure 6. The t-SNE [31] visualization of baseline and ours clustering results on same samples. Samples with the same color in both graphs have the same ground true label. The uppermost portion split by the baseline’s horizontal partitioning is shown on the left, while the top portion masks extracted by our method are shown on the right. Typical samples (a) and (b) have the same ID, while (1) - (6) are from other IDs. The red and green circled regions show that samples mixed in the baseline are separated in our method.

baseline to extract part features mainly contains the background. This results in a person with different labels incorrectly clustered due to the background similarity. In contrast, our method focuses on discriminative head features of the person with the masks obtained through self-learning parsing, making distinguishing persons with different identities more precise. From Fig. 6, it can be observed that for those samples mixed into other clusters, we can generally find their actual categories using our method and maintain the original clustering more closely and cleanly.

4.4. Comparison with State-of-the-Arts

We compare the proposed SCWM with various state-of-the-art unsupervised person re-ID methods on two standard datasets, e.g. Market-1501 and MSMT17. All results are shown in Tab. 4. For fairness, we also test the performance of the PPLR [8] and ISE [45] methods on our backbone separately, and the results are marked with asterisks in the table. From the table, it can be seen that our proposed SCWM method surpasses most previous unsupervised methods, in-

Method	Reference	Market-1501				MSMT17			
		mAP	R1	R5	R10	mAP	R1	R5	R10
<i>Purely Unsupervised</i>									
BUC [20]	AAAI'19	38.3	66.2	79.6	84.5	-	-	-	-
MMCL [32]	CVPR'20	45.5	80.3	89.4	92.3	11.2	35.4	44.8	49.8
HCT [43]	CVPR'20	56.4	80.0	91.6	95.2	-	-	-	-
MMT [12]	ICLR'20	74.3	88.1	96.0	97.5	-	-	-	-
SpCL [13]	NeurIPS'20	73.1	88.1	95.1	97.0	19.1	42.3	56.5	68.4
GCL [4]	CVPR'21	66.8	87.3	93.5	95.5	21.3	45.7	58.6	64.5
ICE [3]	ICCV'21	79.5	92.0	97.0	98.1	29.8	59.0	71.7	77.0
RLCC [44]	CVPR'21	77.7	90.8	96.3	97.5	27.9	56.5	68.4	73.1
MCRN [37]	AAAI'22	80.8	92.5	-	-	31.2	63.6	-	-
CCL [9]	ACCV'22	82.1	92.3	96.7	97.9	27.6	56.0	66.8	71.5
PPLR [8]	CVPR'22	81.5	92.8	97.1	98.1	31.4	61.1	73.4	77.8
ISE [45]	CVPR'22	84.7	94.0	97.8	98.8	35.0	64.7	75.5	79.4
ISE*	-	87.6	95.3	<u>98.2</u>	<u>98.9</u>	<u>46.4</u>	<u>74.9</u>	<u>84.3</u>	<u>87.5</u>
PPLR* (Baseline)	-	86.6	94.5	98.0	98.7	46.1	73.4	83.7	87.0
Our SCWM*	This paper	<u>87.5</u>	<u>94.9</u>	98.4	99.0	49.1	76.5	85.4	88.4
<i>Supervised</i>									
PCB [29]	ECCV'18	81.6	93.8	97.5	98.5	40.4	68.2	-	-
ISP [50]	ECCV'20	88.6	95.3	98.6	-	-	-	-	-
ABD-Net [5]	ICCV'19	88.3	95.6	-	-	60.8	82.3	-	-
ISE (w/ ground-truth) [45]	CVPR'22	87.8	95.6	98.5	99.2	51.0	76.8	87.1	90.6
Our SCWM* (w/ ground-truth)	This paper	88.1	95.3	98.3	99	60.4	82.3	90.4	92.7

Table 4. Comparison with state-of-the-art re-ID methods on Market-1501 and MSMT17 datasets. The first and second best results among all unsupervised methods are marked in **bold** and underlined, respectively. * denotes the backbone settings with SYNTH-PEDES pretrained ResNet-50.

cluding BUC [20], MMCL [32], HCT [43], MMT [12], GCL [4], ICE [3], SpCL [13], RLCC [44], MCRN [37], CCL [9], and PPLR [8]. In addition, compared to supervised part-based methods, we have also achieved similar performance. Only PPLR, PCB [29], ISP [50], and our SCWM in the table are part-based methods, and others only focus on global features. Among these part-based methods, only we individually apply metric learning to each part feature. PPLR and PCB do not utilize metric learning, while ISP concatenates all part features for metric learning. ISE [45] proposes a method for sample augmentation in the feature space. However, our backbone already provides good clustering features, which narrows the gap between ISE and other methods. Therefore, our method surpasses them by being able to extract and leverage more abundant local information. As shown in Tab. 4, our method surpasses the baseline method on all the benchmarks with +0.9% and 3.0% of mAP on Market-1501 and MSMT17, respectively. On MSMT17, our method significantly outperforms the prior state-of-the-art method [45] with 2.7% higher in mAP. In addition, we also test the results of our method with ground true labels. As shown in the lower block of Tab. 4, our method is competitive with previous supervised part-based methods and surpass ISE [45] with

ground truth. Our method achieves a similar performance to ABD-Net in the supervised setting. These results indicate that our method is also applicable to supervised re-ID tasks.

5. Conclusion

In part-based unsupervised person re-identification methods, the primary challenges stem from misalignment and noise of part features. To address these two issues, we introduced self-learning human parsing with spatial cascaded clustering, which allows part features to be semantically aligned and improves the precision of part feature segmentation to reduce noise. We analyzed two limitations of the cascaded clustering method used in current approaches: foreground omissions and spatial confusions. We proposed foreground and space correction, significantly improving the parsing performance. After aligning part features, we revised the memory module based on the proposed assumptions and requirements to better learn and leverage part features. We propose a weighted memory with a flexible weighted update strategy considering hard example mining and noise suppression. Experiments' results show that our method has achieved almost the best performance compared to state-of-the-art methods.

References

- [1] M Caron, I Misra, J Mairal, P Goyal, P Bojanowski, and A Joulin. Unsupervised learning of visual features by contrasting cluster assignments. *Advances in Neural Information Processing Systems*, 33:9912–9924, 2020. [2](#)
- [2] Binghui Chen, Weihong Deng, and Jiani Hu. Mixed high-order attention network for person re-identification. In *2019 IEEE/CVF International Conference on Computer Vision (ICCV)*, 2019. [2](#)
- [3] Hao Chen, Benoit Lagadec, and Francois Bremond. Ice: Inter-instance contrastive encoding for unsupervised person re-identification. In *Proceedings of the IEEE/CVF International Conference on Computer Vision*, pages 14960–14969, 2021. [1](#), [8](#)
- [4] Hao Chen, Yaohui Wang, Benoit Lagadec, Antitza Dantcheva, and Francois Bremond. Joint generative and contrastive learning for unsupervised person re-identification. In *2021 IEEE/CVF Conference on Computer Vision and Pattern Recognition (CVPR)*, page 8. IEEE, 2021. [8](#)
- [5] Tianlong Chen, Shaojin Ding, Jingyi Xie, Ye Yuan, Wuyang Chen, Yang Yang, Zhou Ren, and Zhangyang Wang. Abdnnet: Attentive but diverse person re-identification. In *Proceedings of the IEEE/CVF international conference on computer vision*, pages 8351–8361, 2019. [8](#)
- [6] T Chen, S Kornblith, M Norouzi, and G Hinton. A simple framework for contrastive learning of visual representations. In *International conference on machine learning*, pages 1597–1607, 2020. [2](#)
- [7] Weihua Chen, Xianzhe Xu, Jian Jia, Hao Luo, Yaohua Wang, Fan Wang, Rong Jin, and Xiuyu Sun. Beyond appearance: a semantic controllable self-supervised learning framework for human-centric visual tasks. In *Proceedings of the IEEE/CVF Conference on Computer Vision and Pattern Recognition*, pages 15050–15061, 2023. [2](#)
- [8] Yoonki Cho, Woo Jae Kim, Seunghoon Hong, and Sung-Eui Yoon. Part-based pseudo label refinement for unsupervised person re-identification. In *Proceedings of the IEEE/CVF Conference on Computer Vision and Pattern Recognition*, pages 7308–7318, 2022. [1](#), [2](#), [4](#), [5](#), [6](#), [7](#), [8](#)
- [9] Zuozhuo Dai, Guangyuan Wang, Weihao Yuan, Siyu Zhu, and Ping Tan. Cluster contrast for unsupervised person re-identification. In *Proceedings of the Asian Conference on Computer Vision*, pages 1142–1160, 2022. [2](#), [3](#), [4](#), [5](#), [6](#), [8](#)
- [10] Martin Ester, Hans-Peter Kriegel, Jörg Sander, and Xiaowei Xu. A density-based algorithm for discovering clusters in large spatial databases with noise. In *KDD*, page 6, 1996. [3](#)
- [11] Hehe Fan, Liang Zheng, Chenggang Yan, and Yi Yang. Unsupervised person re-identification. *ACM Transactions on Multimedia Computing, Communications, and Applications*, 14(4):1–18, 2018. [1](#)
- [12] Yixiao Ge, Dapeng Chen, and Hongsheng Li. Mutual mean-teaching: Pseudo label refinery for unsupervised domain adaptation on person re-identification. *arXiv preprint arXiv:2001.01526*, 2020. [1](#), [8](#)
- [13] Yixiao Ge, Feng Zhu, Dapeng Chen, Rui Zhao, et al. Self-paced contrastive learning with hybrid memory for domain adaptive object re-id. *Advances in Neural Information Processing Systems*, 33:11309–11321, 2020. [1](#), [2](#), [4](#), [6](#), [8](#)
- [14] Jianyuan Guo, Yuhui Yuan, Lang Huang, Chao Zhang, Jin-Ge Yao, and Kai Han. Beyond human parts: Dual part-aligned representations for person re-identification. In *2019 IEEE/CVF International Conference on Computer Vision (ICCV)*, 2019. [2](#)
- [15] R Hadsell, S Chopra, and Y Lecun. Dimensionality reduction by learning an invariant mapping. In *2006 IEEE Computer Society Conference on Computer Vision and Pattern Recognition - Volume 2 (CVPR'06)*, pages 1735–1742. IEEE, 2006. [2](#)
- [16] Kaiming He, Xiangyu Zhang, Shaoqing Ren, and Jian Sun. Deep residual learning for image recognition. In *2016 IEEE Conference on Computer Vision and Pattern Recognition (CVPR)*, number 6. IEEE, 2016. [5](#)
- [17] Kaiming He, Haoqi Fan, Yuxin Wu, Saining Xie, and Ross Girshick. Momentum contrast for unsupervised visual representation learning. In *2020 IEEE/CVF Conference on Computer Vision and Pattern Recognition (CVPR)*, pages 9729–9738. IEEE, 2020. [2](#)
- [18] Dangwei Li, Xiaotang Chen, Zhang Zhang, and Kaiqi Huang. Learning deep context-aware features over body and latent parts for person re-identification. In *2017 IEEE Conference on Computer Vision and Pattern Recognition (CVPR)*, pages 384–393, 2017. [2](#)
- [19] Wei Li, Xiatian Zhu, and Shaogang Gong. Harmonious attention network for person re-identification. In *2018 IEEE/CVF Conference on Computer Vision and Pattern Recognition*, pages 2285–2294, 2018. [2](#)
- [20] Yutian Lin, Xuanyi Dong, Liang Zheng, Yan Yan, and Yi Yang. A bottom-up clustering approach to unsupervised person re-identification. *Proceedings of the AAAI Conference on Artificial Intelligence*, 33(01):8738–8745, 2019. [1](#), [8](#)
- [21] Jinxian Liu, Bingbing Ni, Yichao Yan, Peng Zhou, Shuo Cheng, and Jianguo Hu. Pose transferrable person re-identification. In *2018 IEEE/CVF Conference on Computer Vision and Pattern Recognition*, pages 4099–4108, 2018. [2](#)
- [22] Rongsheng Luo, Rukai Wei, Changxin Gao, and Nong Sang. Frequency information matters for image matting. In *Asian Conference on Pattern Recognition*, pages 81–94. Springer, 2023. [2](#)
- [23] Thomas Mauthner, Horst Possegger, Georg Waltner, and Horst Bischof. Encoding based saliency detection for videos and images. In *Proceedings of the IEEE Conference on Computer Vision and Pattern Recognition*, pages 2494–2502, 2015. [4](#)
- [24] Jiaxu Miao, Yu Wu, Ping Liu, Yuhang Ding, and Yi Yang. Pose-guided feature alignment for occluded person re-identification. In *2019 IEEE/CVF International Conference on Computer Vision (ICCV)*, pages 542–551, 2019. [2](#)
- [25] Ishan Misra and Laurens Van Der Maaten. Self-supervised learning of pretext-invariant representations. In *2020 IEEE/CVF Conference on Computer Vision and Pattern Recognition (CVPR)*, pages 6707–6717. IEEE, 2020. [2](#)
- [26] M Sarfraz, Arne Schumann, Andreas Eberle, and Rainer Stiefelwagen. A pose-sensitive embedding for person re-identification with expanded cross neighborhood re-ranking.

- In *2018 IEEE/CVF Conference on Computer Vision and Pattern Recognition*, pages 420–429, 2018. 2
- [27] Jianlou Si, Honggang Zhang, Chun-Guang Li, Jason Kuen, Xiangfei Kong, Alex Kot, and Gang Wang. Dual attention matching network for context-aware feature sequence based person re-identification. In *2018 IEEE/CVF Conference on Computer Vision and Pattern Recognition*, pages 5363–5372, 2018. 2
- [28] Chunfeng Song, Yan Huang, Wanli Ouyang, and Liang Wang. Mask-guided contrastive attention model for person re-identification. In *2018 IEEE/CVF Conference on Computer Vision and Pattern Recognition*, pages 1179–1188, 2018. 2
- [29] Yifan Sun, Liang Zheng, Yi Yang, Qi Tian, and Shengjin Wang. Beyond part models: Person retrieval with refined part pooling (and a strong convolutional baseline). In *Proceedings of the European conference on computer vision (ECCV)*, pages 480–496, 2018. 2, 4, 5, 8
- [30] Yonglong Tian, Dilip Krishnan, and Phillip Isola. Contrastive multiview coding. In *Computer Vision – ECCV 2020*, pages 776–794. Springer International Publishing, 2020. 2
- [31] Laurens Van Der Maaten and Geoffrey Hinton. Visualizing data using t-sne. *Journal of Machine Learning Research (JMLR)*, 4:7, 2008. 7
- [32] Dongkai Wang and Shiliang Zhang. Unsupervised person re-identification via multi-label classification. In *2020 IEEE/CVF Conference on Computer Vision and Pattern Recognition (CVPR)*, pages 10981–10990. IEEE, 2020. 1, 8
- [33] Guanshuo Wang, Yufeng Yuan, Xiong Chen, Jiwei Li, and Xi Zhou. Learning discriminative features with multiple granularities for person re-identification. In *Proceedings of the 26th ACM international conference on Multimedia*, pages 274–282, 2018. 5
- [34] Menglin Wang, Baisheng Lai, Jianqiang Huang, Xiaojin Gong, and Xian-Sheng Hua. Camera-aware proxies for unsupervised person re-identification. *Proceedings of the AAAI Conference on Artificial Intelligence*, 35(4):2764–2772, 2021. 1
- [35] Longhui Wei, Shiliang Zhang, Wen Gao, and Qi Tian. Person transfer gan to bridge domain gap for person re-identification. In *2018 IEEE/CVF Conference on Computer Vision and Pattern Recognition*, page 5. IEEE, 2018. 5
- [36] Qiong Wu, Pingyang Dai, Jie Chen, Chia-Wen Lin, Yongjian Wu, Feiyue Huang, Bineng Zhong, and Rongrong Ji. Discover cross-modality nuances for visible-infrared person re-identification. In *Proceedings of the IEEE/CVF Conference on Computer Vision and Pattern Recognition*, pages 4330–4339, 2021. 2
- [37] Yuhang Wu, Tengpeng Huang, Haotian Yao, Chi Zhang, Yuanjie Shao, Chuchu Han, Changxin Gao, and Nong Sang. Multi-centroid representation network for domain adaptive person re-id. In *Proceedings of the AAAI Conference on Artificial Intelligence*, pages 2750–2758, 2022. 2, 6, 8
- [38] Zhirong Wu, Yuanjun Xiong, Stella Yu, and Dahua Lin. Unsupervised feature learning via non-parametric instance discrimination. In *2018 IEEE/CVF Conference on Computer Vision and Pattern Recognition*. IEEE, 2018. 2
- [39] Shiyu Xuan and Shiliang Zhang. Intra-inter camera similarity for unsupervised person re-identification. In *2021 IEEE/CVF Conference on Computer Vision and Pattern Recognition (CVPR)*, pages 11926–11935. IEEE, 2021. 1
- [40] Wenjie Yang, Houjing Huang, Zhang Zhang, Xiaotang Chen, Kaiqi Huang, and Shu Zhang. Towards rich feature discovery with class activation maps augmentation for person re-identification. In *2019 IEEE/CVF Conference on Computer Vision and Pattern Recognition (CVPR)*, pages 1389–1398, 2019. 2
- [41] Hantao Yao, Shiliang Zhang, Richang Hong, Yongdong Zhang, Changsheng Xu, and Qi Tian. Deep representation learning with part loss for person re-identification. *IEEE Transactions on Image Processing*, 28:2860–2871, 2019. 2
- [42] Mang Ye, Xu Zhang, Pong Yuen, and Shih-Fu Chang. Unsupervised embedding learning via invariant and spreading instance feature. In *2019 IEEE/CVF Conference on Computer Vision and Pattern Recognition (CVPR)*, pages 6210–6219. IEEE, 2019. 2
- [43] Kaiwei Zeng, Munan Ning, Yaohua Wang, and Yang Guo. Hierarchical clustering with hard-batch triplet loss for person re-identification. In *2020 IEEE/CVF Conference on Computer Vision and Pattern Recognition (CVPR)*. IEEE, 2020. 8
- [44] Xiao Zhang, Yixiao Ge, Yu Qiao, and Hongsheng Li. Refining pseudo labels with clustering consensus over generations for unsupervised object re-identification. In *Proceedings of the IEEE/CVF Conference on Computer Vision and Pattern Recognition*, pages 3436–3445, 2021. 1, 8
- [45] Xinyu Zhang, Dongdong Li, Zhigang Wang, Jian Wang, Errui Ding, Javen Qinfeng Shi, Zhaoxiang Zhang, and Jingdong Wang. Implicit sample extension for unsupervised person re-identification. In *Proceedings of the IEEE/CVF Conference on Computer Vision and Pattern Recognition*, pages 7369–7378, 2022. 1, 4, 6, 7, 8
- [46] Feng Zheng, Cheng Deng, Xing Sun, Xinyang Jiang, Xiaowei Guo, Zongqiao Yu, Feiyue Huang, and Rongrong Ji. Pyramidal person re-identification via multi-loss dynamic training. In *Proceedings of the IEEE/CVF conference on computer vision and pattern recognition*, pages 8514–8522, 2019. 2
- [47] Liang Zheng, Liyue Shen, Lu Tian, Shengjin Wang, Jingdong Wang, and Qi Tian. Scalable person re-identification: A benchmark. In *2015 IEEE International Conference on Computer Vision (ICCV)*, number 5. IEEE, 2015. 5
- [48] Ruochen Zheng, Lerenhan Li, Chuchu Han, Changxin Gao, and Nong Sang. Camera style and identity disentangling network for person re-identification. In *BMVC*, page 66, 2019. 2
- [49] Yi Zheng, Shixiang Tang, Guolong Teng, Yixiao Ge, Kaijian Liu, Jing Qin, Donglian Qi, and Dapeng Chen. Online pseudo label generation by hierarchical cluster dynamics for adaptive person re-identification. In *2021 IEEE/CVF International Conference on Computer Vision (ICCV)*, pages 8371–8381. IEEE, 2021. 1
- [50] Kuan Zhu, Haiyun Guo, Zhiwei Liu, Ming Tang, and Jinqiao Wang. Identity-guided human semantic parsing for person re-identification. In *Computer Vision–ECCV 2020: 16th*

European Conference, Glasgow, UK, August 23–28, 2020, Proceedings, Part III 16, pages 346–363. Springer, 2020. [1](#), [2](#), [4](#), [6](#), [7](#), [8](#)

- [51] Jialong Zuo, Changqian Yu, Nong Sang, and Changxin Gao. Plip: Language-image pre-training for person representation learning, 2023. [6](#)